

## Article

# Density, Viscosity, Refractive Index, Speed of Sound, Molar Volume, Isobaric Thermal Compressibility, Excess Gibbs Activation for Fluid Flow, and Isentropic Compressibility of Binary Mixtures of Methanol with Anisole and with Toluene at 298.15 K and 0.1 MPa

Hannah S. Slocumb and Gerald R. Van Hecke \*

Department of Chemistry, Harvey Mudd College, Claremont, CA 91711, USA; hslocumb@g.hmc.edu

\* Correspondence: vanhecke@g.hmc.edu

**Abstract:** Density, viscosity, refractive index, and ultrasonic velocity were measured for the pure materials anisole, methanol, and toluene, and for the binary mixtures: methanol–anisole and methanol–toluene. Excess molar volume  $V^E$ , isobaric thermal compressibility  $\alpha$ , excess Gibbs activation energy for fluid flow  $\Delta G^{E*}$ , and excess isentropic compressibility  $\kappa_S^E$  were calculated from the measured quantities. For both binary mixtures  $V^E$  and  $\kappa_S^E$  were  $<0$  while  $\Delta n > 0$  and  $\Delta G^{E*} > 0$  over the entire mole fraction composition range. Anisole mixtures exhibited more negative values for  $V^E$  and  $\kappa_S^E$  while more positive values were displayed for  $\Delta n$  and  $\Delta G^{E*}$  compared to toluene mixtures. For  $\Delta\eta$ , negative values were observed at low alcohol concentrations but positive values at high alcohol concentrations for both systems.

**Keywords:** small molecule liquid mixtures; physical properties; molar volume; isentropic compressibility; refractive index



**Citation:** Slocumb, H.S.; Van Hecke, G.R. Density, Viscosity, Refractive Index, Speed of Sound, Molar Volume, Isobaric Thermal Compressibility, Excess Gibbs Activation for Fluid Flow, and Isentropic Compressibility of Binary Mixtures of Methanol with Anisole and with Toluene at 298.15 K and 0.1 MPa. *Liquids* **2024**, *4*, 402–414. <https://doi.org/10.3390/liquids4020021>

Academic Editors: Cory Pye and Enrico Bodo

Received: 27 December 2023

Revised: 17 April 2024

Accepted: 1 May 2024

Published: 10 May 2024



**Copyright:** © 2024 by the authors. Licensee MDPI, Basel, Switzerland. This article is an open access article distributed under the terms and conditions of the Creative Commons Attribution (CC BY) license (<https://creativecommons.org/licenses/by/4.0/>).

## 1. Introduction

Binary mixtures of low molecular weight liquids such as alcohols and aromatics have been extensively studied not only to provide fundamental physical property data but also to test the influence of molecular structure, polarity, and size on measured properties [1–3]. Binary mixtures have also provided data to develop mixing rules and test fitting models for excess volume and viscosity increment [4–6]. This study presents data on mixtures of the highly polar aliphatic alcohol methanol with a polar aromatic compound anisole with a weakly polar aromatic toluene. Does methanol interact with polar aromatic anisole more than with the essentially non-polar aromatic toluene to cause greater specific interactions either of a dipole–dipole or H-bonded nature in their mixtures? All of the subject compounds are used as solvents for various reactions, especially methanol and toluene. Their physical properties are thus of interest for chemical and engineering applications [7]. Anisole has been suggested as a “green solvent” to replace toluene in some applications [8].

The density, viscosity, refractive indices, and the speed of sound were measured for anisole–methanol and anisole–toluene mixtures at 298.15 K and 0.1 MPa. From this data, the excess volume  $V^E$ , excess isentropic compressibility  $\kappa_S^E$ , excess Gibbs activation energy for viscous flow  $\Delta G^{E*}$ , deviations in viscosity  $\Delta\eta$ , and refractive index  $\Delta n$  were calculated. In addition, the isobaric coefficient of thermal expansion  $\alpha$  for anisole–methanol mixtures was calculated.

Non-ideality in these mixtures was estimated from simple linear mixing rules and expressed as either excess or increment quantities. While more complex mixing rules exist for some of the properties, it is believed that the simple linear rule satisfactorily discovers

the existence of non-ideality in the mixtures. The aim of this work was not to test theoretical models describing liquid mixtures.

The trends in the excess or deviation values are related to the molecular structures and the physical properties of the three components.

## 2. Experimental Section

Material sources are listed in Table 1. All measurements were made under ambient atmospheric pressure, measured with mercury in a glass barometer. During the course of the measurements, the laboratory pressure varied between 726 and 731 Torr or 0.0968 and 0.0975 MPa, which averages to one significant figure as 0.1 MPa with a range of about 0.0007 MPa. The standard deviation in this average would estimate the uncertainty to be  $\pm 0.0005$  MPa.

**Table 1.** Materials.

Compound	CAS	Source	Molecular Mass/g mol <sup>-1</sup>	Purity	Purification
Anisole	100-66-3	Aldrich, Analytical Standard	108.140	99.7%	Fractional distillation
Methanol	67-56-1	Spectrum ACS Reagent grade	32.04	>99.9%	Distilled over CaH <sub>2</sub>
Toluene	108-88-3	Spectrum ACS Reagent grade	92.141	99.5%	Used as received
Water	7732-18-5	Anton Paar Ultrapure certified	18.02		Used as received

Solutions of reagents were made in approximately 0.1 mole fraction increments. Approximate volumes of samples were syringed into capped bottles and then massed to  $\pm 0.1$  mg without buoyancy corrections to determine mole fractions. The mole fractions are precise to at least  $\pm 0.00003$ .

Density data were collected using an Anton Parr densitometer using the Pulsed Excitation Method (model DMA 4500A) with Peltier temperature control good to  $\pm 0.05$  K. Density measurements were performed at 298.15 K and 0.1 MPa for methanol–toluene mixtures and over the range of 288.15–318.15 K at 0.1 MPa in 10 K increments in the case of anisole–toluene mixtures. The densitometer U-tube was loaded using a syringe that was cleaned after each sample measurement by pushing reagent ethanol through the U-tube, followed by air drying until the air density in the tube was steady for at least a minute. Sample temperatures were allowed to equilibrate to within  $\pm 0.05$  °C of the target temperature before measurements were made. Calibration of the instrument followed the procedure recommended by the manufacturer, using ultra-pure water from Anton Paar. Density values gave standard deviations of at most  $\pm 0.02$  kg m<sup>-3</sup>. The density results for the pure materials may be found in Table 2. Agreement with the literature values for the pure materials is excellent. The results for the mixtures may be found in Table 3.

The Anton Paar Lovis 2000 Microviscometer attached to the DMA 4500 A was used to measure dynamic viscosity with Peltier temperature control good to  $\pm 0.05$  K. Measurements were made at 298.15 K and 0.1 MPa. Samples were manually inserted into the rolling ball capillary by syringe rather than using a flow-through procedure. The vapor pressure of methanol is high enough that the flow-through method often results in bubbles in the capillary. Measurements were only made with bubble-free capillaries. A 1.59 mm diameter capillary was used with a steel ball. The capillary and ball were cleaned with ethanol between samples and then air dried until the ball rolled smoothly in the capillary. Temperature equilibration was achieved within  $\pm 0.01$  °C of the target temperature before measurements were made. Viscosity values gave a standard deviation of at most  $\pm 0.002$  mPa s. Anton Paar Ultrapure water was used for calibration as recommended by the manufacturer. The viscosity results for the pure materials may be found in Table 2. Agreement with the literature values for the pure materials is excellent. The results for the mixtures may be found in Table 3.

Refractive indices were measured at 298.15 K and 0.1 MPa using an Anton Paar automatic refractometer model Abbemat WR-MW using 589.3 nm light (Na D line) with

temperature control ( $\pm 0.05$  K) provided by the built-in Peltier heating/cooling system. The laser was allowed to warm up for at least a half hour, at which time the instrument was calibrated using Anton Paar Ultrapure water as recommended by the manufacturer. The prism was cleaned between each sample by wiping the prism with pure ethanol using a chemical wipe and air dried. To avoid composition changes due to evaporation, measurements were made as soon as the sample chamber was sealed and at the temperature reached within  $\pm 0.03$  °C of the target. The refractive index measurements gave standard deviations of no more than  $\pm 0.00003$ . The refractive index results for the pure materials may be found in Table 2. Agreement with the literature values for the pure materials is excellent. The results for the mixtures may be found in Table 3.

The speed of sound was measured using a Mittal Enterprises Model M-81 F Multifrequency Ultrasonic Interferometer (New Patel Nagar, Delhi, 110008 India). All measurements were made at 2 MHz. The cell was carefully dried between measurements. Temperature was controlled to  $\pm 0.05$  °C by an external circulating water bath (Neslab model RTE 100). Typical standard deviation of the frequency maxima was  $\pm 0.002$ . The ultrasound results for the pure materials may be found in Table 2. The results for the mixtures may be found in Table 3. There is excellent agreement with the literature values.

### 3. Data Treatment

The excess volumes were calculated using the traditional expression Equation (1),

$$V^E = \frac{M_1x_1 + M_2x_2}{\rho_{meas}} - \left[ \frac{M_1x_1}{\rho_1} + \frac{M_2x_2}{\rho_2} \right] \quad (1)$$

where  $\rho_{meas}$  is the measured density of the solution of interest;  $M_i$  and  $\rho_i$  are the molar mass and density of the pure compounds. The molar fraction  $x_i$  defines the solution composition.

The ultrasound velocity  $c$  was calculated using Equation (2),

$$c = \lambda \cdot f \quad (2)$$

where  $f$  is the frequency of the interferometer in  $s^{-1}$  and  $\lambda$  is the wavelength of the standing wave in the interferometer determined by  $2 \times$  the distance between consecutive signal maxima.

The isentropic compressibility was calculated by Equation (3),

$$\kappa_S = \frac{1}{c^2 \times \rho} \quad (3)$$

where  $c$  is the ultrasound velocity and  $\rho$  is the density of the liquid mixture.

The isobaric coefficient of thermal expansion  $\alpha$  was calculated using Equation (4) from the variation in the  $\ln(\text{density})$  with temperature data.

$$\alpha = - \left( \frac{\partial \ln \rho}{\partial T} \right)_p \quad (4)$$

A deviation from ideality in the measured property  $z$  for a mixture is defined here as  $\Delta z$ , which may represent either an excess value or incremental value and was calculated via Equation (5),

$$\Delta z = z_{meas} - [x_1z_1 + x_2z_2] \quad (5)$$

where  $x_i$  and  $z_i$  are the molar fraction of a component in the mixture and the physical property of a pure component, respectively. This simple linear mixing rule was used for all deviation calculations and its use is very common in the literature, for example, Joshi et al. [1], Rattan et al. [2], and Weng [3].

The excess Gibbs energy of activation for viscous flow was calculated from volume and viscosity data using Equation (6) [9,10],

$$\Delta G^{E*} = RT \left[ \ln(V\eta) - \sum_{i=1}^2 x_i \ln(V_i \eta_i) \right] \quad (6)$$

where  $R$  and  $T$  have their usual meaning and  $V$  is the molar volume of the solution whose dynamic viscosity is  $\eta$ . Further  $x_i$ ,  $V_i$ , and  $\eta_i$  are, respectively, the mole fraction, molar volume, and dynamic viscosity of the pure components.

The excess and deviation data were correlated to the molar fraction of the mixture using a Redlich–Kister polynomial Equation (7) [11].

$$z^E(x) \text{ or } \Delta z(x) = (1-x)x \sum_{i=0} A_i (1-2x)^i \quad (7)$$

The  $A_i$  coefficients were determined using a least-squares matrix regression method available in the program PTC Mathcad Prime 4.0 [and earlier versions]. Three terms in the polynomial, fourth order in composition, were found to be sufficient to describe the deviation data in terms of the calculated standard deviation of the fit, calculated by Equation (8), and visual observation,

$$\sigma = \sqrt{\frac{\sum_i (z(x_i) - z_{fit}(x_i))^2}{n - w}} \quad (8)$$

where  $n$  is the number of data points and  $w$  is the number of coefficients in the correlating equation. It should be noted that  $w$  is one less than the highest order of the composition molar fraction so if  $w = 4$ , the highest order in molar fraction would be 5.

The fitting coefficients for the mixtures may be found in Table 4.

#### 4. Results and Discussion

The excellent agreement between the measure values and the literature reflects the success of the calibration methods used with modern instruments as shown in Table 2.

**Table 2.** Comparison of the measured and the literature properties of pure liquids at 298.15 K and 0.1 MPa <sup>a</sup>.

	Methanol		Toluene		Anisole	
	Measured	Literature	Measured	Literature	Measured	Literature
$\rho/\text{kg m}^{-3}$	787.33	787.03 [1]	862.12	862.19 [12] 862.20 [13] <sup>c</sup>	989.13	989.32 [1,14] 988.9 [15]
$V_m/10^{-22} \text{ cm}^3 \text{ molecule}^{-1}$	0.676 <sup>b</sup>		1.78 <sup>b</sup>		1.81 <sup>b</sup>	
$n_D$ [589.3 nm]	1.32658	1.3267 [16] 1.32652 [14]	1.49367	1.49413 [17] 1.4399 [12]	1.51416	1.5148 [18]
$\eta/\text{mPa s}$	0.5522	0.5509 [1] 0.5526 [19]	0.5574	0.5563 [20] <sup>d</sup>	0.9986	0.992 [18]
$c/\text{m s}^{-1}$	1105	1097 [21]	1303	1305.3 [17]	1410	1410 [18]
$\kappa_S/10^{-10} \text{ Pa}^{-1}$	10.380	10.558 [21] <sup>e</sup>	6.822	6.81 [17]	5.080	5.086 [18] <sup>f</sup>
Dipole moment/Debye		1.7 [22]		0.333 [23]		1.26 [15]

<sup>a</sup> Standard uncertainties are  $u(T) = 0.01 \text{ K}$ ,  $u(n) = 0.00001$ ,  $u(\rho) = 0.02 \text{ kg m}^{-3}$ ,  $u(\eta) = 0.0001 \text{ mPa}\cdot\text{s}$ ,  $u(\kappa_S) = 0.002 \cdot 10^{-10} \text{ Pa}^{-1}$ ,  $u(c) = 1.2 \text{ m}\cdot\text{s}^{-1}$ . Expanded uncertainties may be taken to be two times the standard uncertainties to give uncertainty estimates at a 95% confidence level. This practice follows that recommended by R. D. Chirico et al. [24]. <sup>b</sup> Calculated from the measured density. <sup>c</sup> From linear interpolation of data in [13]. <sup>d</sup> From linear interpolation of data in [20]. <sup>e</sup> Calculated from data in [21]. <sup>f</sup> Calculated from data in [17].

Below, in order of presentation, are the  $\Delta n$ ,  $V^E$ ,  $\alpha$ ,  $\Delta\eta$ ,  $\Delta G^{E*}$ , and  $\kappa_S^E$  values derived from the physical properties of the methanol–anisole and methanol–toluene mixtures reported in Table 3. The deviations from ideal behavior are plotted in the appropriate section below and found in Figures 1, 2, and 5–7.

**Table 3.** Density  $\rho$ , Refractive index  $n$  (589.3 nm), Viscosity  $\eta$ , Ultrasound Velocity  $c$ , and Isentropic Compressibility  $\kappa_S$  for mixtures of Methanol–Anisole and Methanol–Toluene at 298.15 K and 0.1 MPa <sup>a</sup>.

$x_{\text{methanol}}$	Methanol–Anisole					$x_{\text{methanol}}$	Methanol–Toluene				
	$\rho/\text{kg}\cdot\text{cm}^{-3}$	$n$	$\eta/\text{mPa}\cdot\text{s}$	$c/\text{m}\cdot\text{s}^{-1}$	$\kappa_S/10^{10}\cdot\text{Pa}^{-1}$		$\rho/\text{kg}\cdot\text{cm}^{-3}$	$n$	$\eta/\text{mPa}\cdot\text{s}$	$c/\text{m}\cdot\text{s}^{-1}$	$\kappa_S/10^{-10}\cdot\text{Pa}^{-1}$
0	989.13	1.51416	0.9986	1410	5.080	0	862.12	1.49367	0.5574	1303	6.822
0.12928	980.33	1.50786	0.9279	1398	5.208	0.09936	859.57	1.48807	0.5455	1293	6.959
0.21053	973.46	1.49937	0.8956	1380	5.398	0.19978	856.18	1.48042	0.5430	1275	7.181
0.31049	963.17	1.48973	0.8621	1369	5.534	0.30247	852.27	1.47102	0.5485	1265	7.332
0.40464	952.54	1.47983	0.8345	1344	5.801	0.40244	847.84	1.46095	0.5573	1244	7.612
0.50692	937.69	1.46902	0.7941	1308	6.232	0.49757	842.78	1.44933	0.5658	1232	7.809
0.60529	919.48	1.44801	0.7554	1291	6.513	0.59884	836.35	1.43560	0.5751	1213	8.117
0.70837	896.92	1.42899	0.7120	1255	7.060	0.69935	828.52	1.41531	0.5788	1200	8.381
0.79938	872.24	1.40372	0.6672	1219	7.740	0.80121	818.07	1.39242	0.5798	1175	8.854
0.90597	833.40	1.37159	0.6070	1176	8.683	0.90000	805.21	1.36376	0.5716	1137	9.615
1	787.33	1.32658	0.5522	1105	10.380	1	787.33	1.32658	0.5522	1105	10.380

<sup>a</sup> Standard uncertainties are  $u(T) = 0.01$  K,  $u(n) = 0.00001$ ,  $u(\rho) = 0.02$  kg m<sup>-3</sup>,  $u(\eta) = 0.0001$  mPa·s,  $u(\kappa_S) = 0.002\cdot 10^{-10}$  Pa<sup>-1</sup>,  $u(c) = 1.2$  m·s<sup>-1</sup>.  $U(T) = 0.02$  K,  $U(n) = 0.00002$ ,  $U(\rho) = 0.04$  kg m<sup>-3</sup>,  $U(\eta) = 0.0002$  mPa·s,  $U(\kappa_S) = 0.004\cdot 10^{-10}$  Pa<sup>-1</sup>,  $U(c) = 2.4$  m·s<sup>-1</sup>. Expanded uncertainties denoted by  $U(\ )$  are taken to be two times the standard uncertainties to give uncertainty estimates at a 95% confidence level. This practice follows that recommended by R. D. Chirico et al. [24].

**Table 4.** The Redlich–Kister coefficients are used in the correlating equations along with the standard deviation of each fit  $\sigma$  using Equation (7).

Property	System	A <sub>0</sub>	A <sub>1</sub>	A <sub>2</sub>	Order	$\sigma$
$V^E/\text{cm}^{-3}\text{mol}^{-1}$	Anisole/methanol	-1.31	0.198	-0.255	4	0.023
	Toluene/methanol	-0.402	0.125	-0.241	4	0.0072
$\Delta n$	Anisole/methanol	0.186	-0.086	0.053	4	0.002
	Toluene/methanol	0.156	-0.066	0.025	4	$5 \times 10^{-4}$
$\Delta\eta/\text{mPa}\cdot\text{s}$	Anisole/methanol	0.092	-0.173	-0.125	4	$2 \times 10^{-3}$
	Toluene/methanol	0.046	-0.204	-0.011	4	$6 \times 10^{-4}$
$\kappa_S^E/10^{-10}\cdot\text{Pa}^{-1}$	Anisole/methanol	-6.33	4.29	-3.94	4	0.075
	Toluene/methanol	-3.16	2.08	-1.12	4	0.047

4.1. Refractive Index Increments

As noted in Figure 1, the refractive indices in the methanol–anisole and methanol–toluene mixtures show positive deviations from ideality,  $\Delta n > 0$ , over the entire composition range. Looking at Figure 2 [below] shows  $V^E < 0$  over the entire composition range for both mixtures. This inversion in ideality  $\Delta n > 0$  while  $V^E < 0$  [or vice versa] is commonly observed, see for example Gonzalez et al. [17] and Iglesias et al. [25].

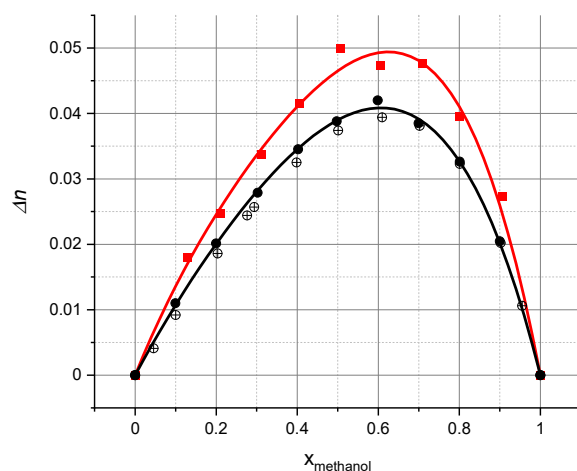


**Figure 1.** Refractive index increments for binary mixtures of methanol with anisole (■) and toluene (●) at 298.15 K and 0.1 MPa versus molar fraction methanol. (/) Methanol–toluene mixtures [18]. The solid lines are data fits using the Redlich–Kister Equation (6).

Furthermore, Iglesias et al. [25] attribute this inversion to the increased dipoles and dispersion effects in a smaller unit volume affecting the passage of light through the medium. Moreover, as  $\Delta n$  for methanol–anisole mixtures is larger—more positive than  $\Delta n$  for methanol–toluene—the  $V^E$  observed for methanol–anisole mixtures should be larger than  $V^E$  in methanol–toluene mixtures. This is observed in Figure 2. It should be noted that anisole has a larger dipole moment compared to toluene and a larger mass, which is associated with increased dispersion effects suggesting the deviation from ideality should be larger in anisole mixtures than in toluene mixtures.

Agreement with the literature values [18] for methanol–toluene mixtures is excellent.

#### 4.2. Molar Volume and Excess Volume

Measurement of excess volume is an excellent and well-studied way to gain insight into how molecules pack and organize in the liquid state. As noted in Figure 2 and Table 5, both the methanol–toluene mixtures and the methanol–anisole mixtures show negative deviations from ideality. This indicates that in mixture, the solutions take up less volume, that is, the molecular components of the mixtures are more attracted to each other for whatever reason in mixture than in pure states. Even though there is some scatter in the methanol–anisole data, it seems clear that  $V^E < 0$ . Mahajan et al. [4] suggest three reasons for observing  $V^E < 0$  in mixtures: (1) weaker dispersion, weak dipole–dipole interactions; (2) clear chemical interactions due to H-bonds; (3) size differences allowing the “solute” to more easily fit into the liquid structure of the majority component.

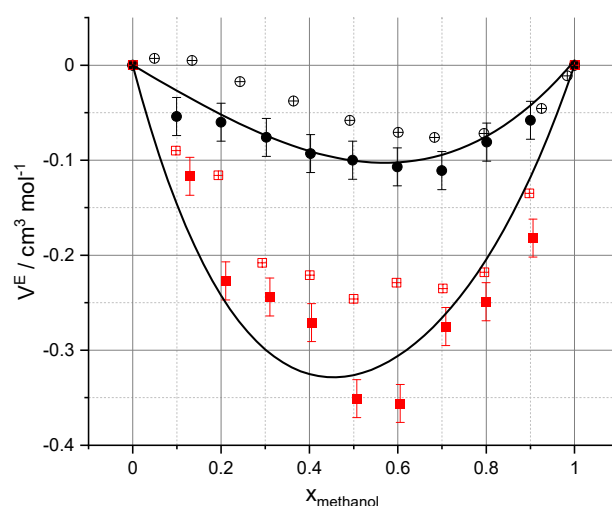


**Figure 2.** Excess volume in binary mixtures at 298.15 K and 0.1 MPa of methanol with anisole (■), and with toluene (●) versus molar fraction of methanol. (◻) Methanol–anisole [1]. (◊) Methanol–toluene [26]. The solid lines are data fits using the Redlich–Kister Equation (6.0).

If it is allowed that methanol forms a loose H-bonded liquid structure, then the presence of either toluene or anisole seems to break up that structure, allowing closer packing of the constituent molecules giving a higher density or negative excess volume. Anisole seems to be more effective in packing in methanol-rich mixtures than toluene. This might appear counterintuitive since anisole is the slightly larger molecule [Table 2 data]; however, the extra conformations possible with the methoxy group of anisole compared to the simple methyl of toluene might make anisole the more effective structure-breaker of the H-bonded methanol. Excess volume in the literature values for methanol–toluene agree with our results in that, by and large,  $V^E < 0$  was observed [26]. The  $V^E$  values noted in Figure 2 show slightly  $>0$  values for very low concentrations of methanol. The  $V^E > 0$  values reported by Ocon et al. [26] for low methanol concentrations are commented on by Srivastava and Smith [26], who note that such weak  $V^E > 0$  are not really representative of

the bulk of methanol–toluene  $V^E$  studies reported in the literature. However, Letcher et al. report small  $V^E > 0$  at low methanol concentrations [27].

Regardless, toluene packs efficiently in high concentrations of methanol to give smaller than expected molar volumes.

There is one report of methanol–anisole  $V^E > 0$  over the entire composition range [28]. Something must be flawed with this result since in the same paper the authors report that the refractive index increments are  $>0$ . As noted above, if  $V^E > 0$ ,  $\Delta n$  increments must be  $<0$ .

#### 4.3. Isobaric Thermal Expansivity for Methanol–Anisole Mixtures at 298.15 K and 0.1 MPa

The  $\ln(\text{density})$ -temperature variation for a given molar fraction was assumed to be linear, which means the isobaric coefficient of thermal expansion is equal to  $-(\partial \ln(\rho)/\partial T)_p$  [Equation (4)], the slope of each line. Figure 3 bears out the assumption of linearity.

The isobaric thermal expansivity values  $\alpha$  derived from the temperature-dependent density values for methanol–anisole mixtures shown in Figure 4 are presented in Table 6.

**Table 5.** Molar volume  $V_m$  and  $V^E$  for binary mixtures of Methanol–Anisole and Methanol–Toluene at 298.15 K and 0.1 MPa<sup>a</sup>.

Methanol–Anisole			Methanol–Toluene		
$x_{\text{methanol}}$	$V_m / \text{cm}^3 \text{mol}^{-1}$	$V^E / \text{cm}^3 \text{mol}^{-1}$	$x_{\text{methanol}}$	$V_m / \text{cm}^3 \text{mol}^{-1}$	$V^E / \text{cm}^3 \text{mol}^{-1}$
0	109.3	0	0	106.9	0
0.12928	100.3	−0.117	0.09936	100.2	−0.054
0.21053	94.63	−0.223	0.19978	93.60	−0.060
0.31049	87.74	−0.244	0.30247	86.78	−0.076
0.40464	81.20	−0.271	0.40244	80.15	−0.093
0.50692	79.19	−0.351	0.49757	73.85	−0.100
0.60529	67.51	−0.356	0.59884	67.14	−0.107
0.70837	60.47	−0.274	0.69935	60.48	−0.111
0.79938	54.24	−0.249	0.80121	53.77	−0.081
0.90597	47.03	−0.182	0.90000	47.26	−0.058
1	40.69	0	1	40.69	0

<sup>a</sup> Standard uncertainty is  $u(x) = 0.0001$ ,  $u(T) = 0.05 \text{ K}$ ,  $u(V_m) = 0.01 \text{ cm}^3 \text{mol}^{-1}$  based on propagated uncertainty. Expanded uncertainty  $U(V_m) = 0.02 \text{ cm}^3 \text{mol}^{-1}$ , implying a 95% confidence level following the recommendation of R. D. Chirico et al. [24].

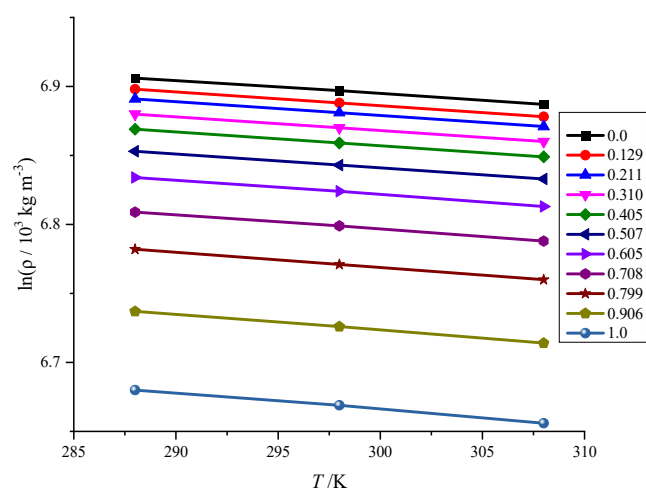


**Figure 3.**  $\ln(\text{density})$  of methanol–anisole mixtures for temperatures from 288.15 K to 308.15 K for specific molar fractions of methanol at 0.1 MPa. The order of the lines from top to bottom follows the molar fractions of methanol given in the side bar legend. The solid lines are assumed linear fits to the data.

**Table 6.** Density of Methanol–Anisole solutions for temperatures from 288.15 K to 308.15 K for specific mole fractions of Methanol at 0.1 MPa. Isobaric thermal expansivity  $\alpha$  and  $\alpha^E$  calculated for 298.15 K and 0.1 MPa for mole fractions of Methanol using Equation (4).

$x_{\text{methanol}}$	$\rho/\text{kg}\cdot\text{m}^{-3}$			$\alpha/10^{-3}\text{ K}^{-1}\text{ }^a$	$\alpha^E/10^{-3}\text{ K}^{-1}$
	288.15 K	298.15 K	308.15 K		
0	998.47	989.13	979.73	1.21	0
0.12928	989.80	980.33	970.74	1.29	0.038
0.21053	982.92	973.47	963.88	1.29	0.012
0.31049	972.65	963.17	953.55	1.29	−0.019
0.40464	962.03	952.55	942.91	1.29	−0.049
0.50692	947.18	937.69	928.04	1.34	−0.032
0.60529	929.06	919.48	909.91	1.35	−0.053
0.70837	906.40	896.92	887.27	1.34	−0.097
0.79938	881.71	872.21	862.61	1.41	−0.056
0.90597	842.83	833.40	823.82	1.47	−0.030
1.000	796.46	787.33	777.65	1.53	0

<sup>a</sup>  $u(\alpha) = 0.02 \cdot 10^{-3}\text{ K}^{-1}$  Expanded uncertainty  $U(\alpha) = 0.04 \cdot 10^{-3}\text{ K}^{-1}$ , implying a 95% confidence level following the recommendation of R. D. Chirico et al. [24].

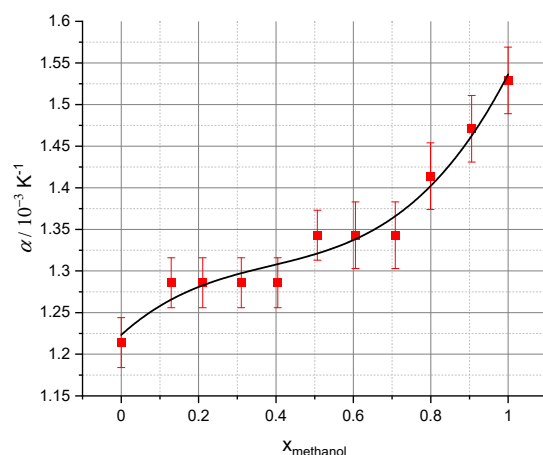


**Figure 4.** The solid line is a cubic fit to  $\alpha$ , the isobaric coefficient of thermal expansion, for methanol–anisole mixtures as function of molar fraction methanol at 298.15 K and 0.1 MPa.

The isobaric thermal expansivity increases with the increase in methanol in the methanol–anisole mixture in a non-linear fashion where  $\alpha^E > 0$ , but quite small, at low concentrations of methanol but  $< 0$  at middle to high concentrations of methanol. The presence of the anisole at higher concentrations of methanol makes the solution less likely to thermally expand, which might follow the increased destruction of the H-bonding in the methanol-rich mixtures.

Since  $\alpha$  is less than ideally predicted for high methanol compositions, the same  $T$  change will expand the solution less, suggesting the intermolecular forces are stronger in the mixture and resist expanding the distance between the molecular components. This is consistent with the negative excess volume where intermolecular distances are smaller than would be expected in an ideal mixture.

#### 4.4. Viscosity Increments

The calculated viscosity increments for both the methanol–toluene and methanol–anisole mixtures agree with the literature, though the methanol–toluene data agreement is better, as shown in Figure 5.

The increment behavior for both mixtures shows both positive and negative deviations from ideality. This is not uncommon behavior for the physical properties of many binary mixtures. The agreement with the literature for the methanol–toluene mixtures  $\alpha$  is excellent.

The difference between the cited literature value for methanol–anisole [2] may be due to the experimental technique used for viscosity—a Ubbelohde viscometer vs. our modern Anton Paar rolling ball viscometer.

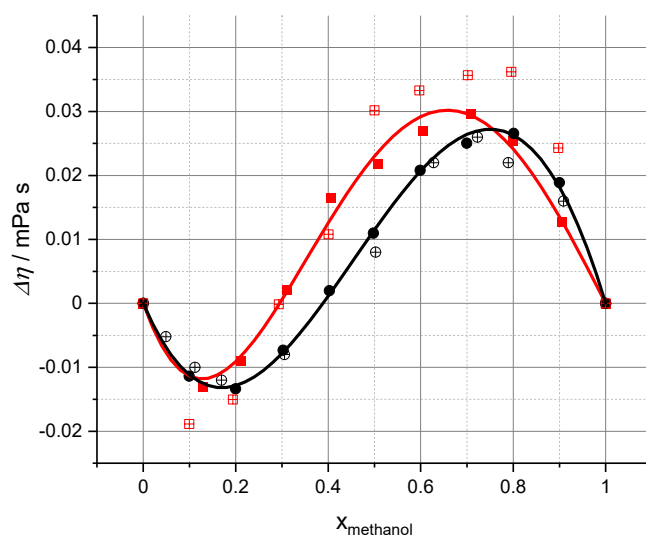


**Figure 5.** Viscosity increments in binary mixtures at 298.15 K and 0.1 MPa of methanol and anisole (■), and with toluene (●) versus molar fraction of methanol. Methanol–anisole mixtures (⊞) [1]. Methanol–toluene (/) mixtures [29]. The solid lines are data fits using the Redlich–Kister Equation (6).

Here the solution behavior shows negative deviations from ideality for low methanol [low alcohol] concentrations but positive deviations for high concentrations of alcohol. Methanol itself has viscosity almost equal to that of toluene but both have a viscosity much lower than anisole [Table 2]. Mialkowski et al. [30] note that  $\Delta\eta < 0$  values occur when dispersion forces are primarily responsible for intermolecular interactions and that  $\Delta\eta$  should be more negative for cases of dipole–dipole interactions which would better describe the more polar methanol–anisole interactions. Roy et al. [31] suggest that when reviewing many binary mixtures, the sign of  $\Delta\eta$  and  $V^E$  are correlated. When,  $V^E < 0$  then  $\Delta\eta < 0$ . Our data do not support that suggestion completely over the entire composition range. In aromatic-rich solutions, both  $V^E < 0$  and  $\Delta\eta < 0$  but at higher methanol concentrations,  $V^E < 0$  while  $\Delta\eta > 0$ . Roy et al. [31] further suggest that where  $\Delta\eta < 0$ , dispersion and dipole interactions are the dominant molecular interactions while  $\Delta\eta > 0$  arises when H-bonding and complex formation are the dominant interactions. Baluja et al. [32] agree with this interpretation suggesting that  $\Delta\eta < 0$  occurs when the molecular interactions between pair of unlike molecules are less than those between like molecules, and moreover,  $\Delta\eta > 0$  occurs when the aromatic component can better form H-bonds with methanol.

#### 4.5. Excess Energy of Viscose Flow

The calculated  $\Delta G^{E*}$  values using the model proposed by Glastone et al. [10] are given in Table 7 and illustrated in Figure 6. The literature report [32] for methanol–anisole deviates from the present data, particularly in higher methanol concentration solutions. This too might be traced to the different instrumentation used to measure density. Since it is clear that  $\Delta G^{E*} > 0$  over the composition range, fitting the data to a Redlich–Kister polynomial would seem to provide no additional information. The  $\Delta G^{E*} > 0$  values over the entire composition range for both systems indicate the viscous flow in these mixtures is more difficult than in the pure liquids. The sign of  $\Delta G^{E*}$  has been taken to indicate existence of intermolecular interactions [1,9,32]. Joshi et al. [1] and Sekhar et al. [9] suggest that when  $\Delta G^{E*} > 0$ , complexes are formed between the molecular components, and the greater the positive value of  $\Delta G^{E*}$ , the stronger the complex. Joshi et al. [1] report for the methanol–anisole mixture a value  $\Delta G^{E*}$  of 485 J mol<sup>−1</sup> but no composition is noted.

This value is roughly in accord with our maximum value for  $\Delta G^{E*}$  observed in Figure 6. Moreover, Joshi et al. [1] report that the methanol–anisole value is larger than that for methanol–benzene. This also seems to be in accord with the anisole mixtures exhibiting larger  $\Delta G^{E*}$  values than toluene mixtures as shown in Figure 6. Prolongo et al. [33] suggest that the sign of  $V^E$  and  $\Delta G^{E*}$  are correlated. The mixtures studied here agree with that suggestion. A comparison to ethanol–anisole mixtures, however, shows that  $\Delta G^{E*} < 0$ , suggesting that size and a dipole have a dramatic influence on  $\Delta G^{E*}$  [34].

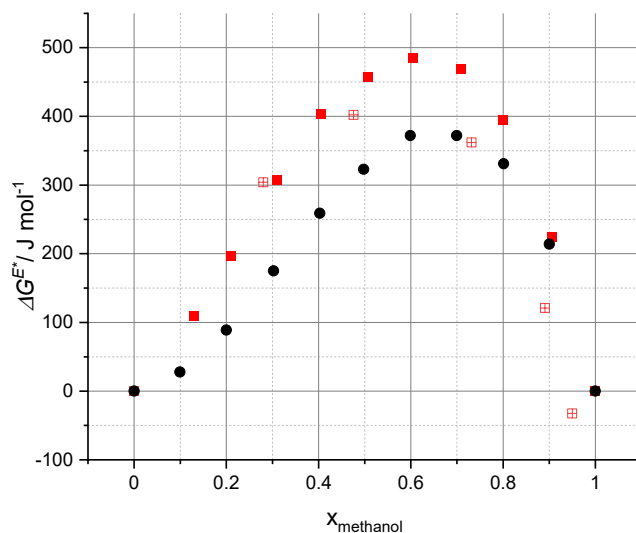


**Figure 6.** Excess Gibbs activation energy  $\Delta G^{E*}$  for viscose flow at 298.15 K and 0.1 MPa for mixtures of methanol–anisole (■), methanol–toluene (●). Methanol–anisole (◻) [32].

**Table 7.** The excess Gibbs activation energy for fluid flow  $\Delta G^{E*}$  at 298.15 K and 0.1 MPa for mixtures of Methanol–Anisole and Methanol–Toluene.

Methanol–Anisole		Methanol–Toluene	
$x_{\text{methanol}}$	$\Delta G^{E*}/\text{J mol}^{-1}$	$x_{\text{methanol}}$	$\Delta G^{E*}/\text{J mol}^{-1}$
0	0	0	0
0.12928	110	0.09936	28
0.21053	197	0.19978	89
0.31049	307	0.30247	175
0.40464	403	0.40244	259
0.50692	457	0.49757	323
0.60529	485	0.59884	372
0.70837	469	0.69935	372
0.79938	395	0.80121	331
0.90597	225	0.90000	214
1.000	0	1	0

$u(\Delta G^{E*}) = 2 \text{ J mol}^{-1}$  with  $U(\Delta G^{E*}) = 4 \text{ J mol}^{-1}$  following the recommendation of Chirico et al. [24].

#### 4.6. Isentropic Compressibilities and Deviations

As noted in Figure 7,  $\kappa_s^E$  values for both methanol–toluene and methanol–anisole mixtures are negative over the entire composition range with  $\kappa_s^E$  for methanol–anisole mixtures everywhere more negative. While the literature agreement with methanol–toluene mixtures is excellent, the literature agreement for methanol–anisole for our data is reasonable for low methanol concentrations, significant differences are observed for high methanol concentrations. The reason for the discrepancy is unknown but probably relates to the different instrumentation used to make the density measurements.

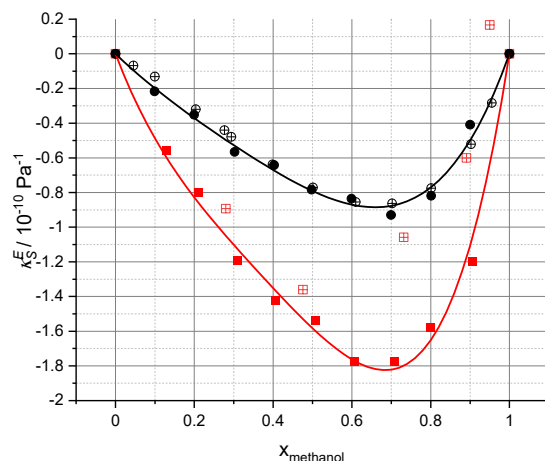


**Figure 7.** Excess isentropic compressibility  $\kappa_S^E$  in binary mixtures at 298.15 K and 0.1 MPa of methanol with anisole (■), and with toluene (●) versus molar fraction of methanol. Methanol–anisole (◻) mixtures [32]. Methanol–toluene (/) mixtures [29]. The solid lines are data fits using the Redlich–Kister Equation (6).

Values of  $\kappa_S^E < 0$  imply the liquid mixture is less easily compressed than either of the pure components, which is consistent with the components mixing together easily to account for the observed  $V^E < 0$  for these mixtures (Sekhar et al. [9]). The excess values for both mixtures show that a small amount of either anisole or toluene has a large effect on  $\kappa_S^E$  and the effect is much greater in methanol–anisole mixtures. Parks et al. [35] have noted that  $\kappa_S^E < 0$  values may be understood by changes in the free volume of the mixture and interstitial accommodation. Further, Nath and Dubey [36] have suggested the H-bonding, dipole–dipole and dipole-induced dipole interactions contribute to negative  $\kappa_S^E$  values. The effect of these interactions should be less for the weaker polar mixtures of methanol–toluene but may be a significant factor in the more polar methanol–anisole mixtures.

## 5. Summary/Conclusions

Several commonly measured physical properties are reported here for binary mixtures of methanol–toluene and methanol–anisole. The differences in the physical properties of the mixtures can be attributed to strong dipole–weak dipole effects in the methanol–toluene system compared to the strong dipole–dipole interactions in the methanol–anisole system as well as significant size differences between the methanol and the aromatic component. The values of,  $V^E$ ,  $\Delta n$ ,  $\Delta G^{E*}$ , and  $\kappa^E$  follow the same curvatures, being either  $>$  or  $<$  0 over the entire composition range with composition with the methanol–anisole system always showing the larger deviation from ideality. However,  $\Delta\eta$  shows “sigmodal” behavior with  $\Delta\eta < 0$  for low methanol concentrations but  $\Delta\eta > 0$  for high methanol concentrations.

**Author Contributions:** Concepts: H.S.S., G.R.V.H.; Data Collection: H.S.S.; Analysis: H.S.S., G.R.V.H.; Supervision: G.R.V.H.; Visualization: H.S.S., G.R.V.H.; Writing original draft: H.S.S.; Writing, review and editing: H.S.S., G.R.V.H. All authors have read and agreed to the published version of the manuscript.

**Funding:** Harvey Mudd College John Stauffer Endowed Fund, Luke Student Research Endowment in Chemistry, NSF Major Research Instrumentation Program Grant GR51005 NSF CHE-1727029.

**Data Availability Statement:** The fundamental data collected are presented in the data tables.

**Conflicts of Interest:** The authors declare no conflicts of interest.

## References

1. Joshi, S.S.; Aminabhavi, T.M.; Shukla, S.S. Densities and viscosities of binary liquid mixtures of anisole with methanol and benzene. *J. Chem. Eng. Data* **1990**, *35*, 187–189. [[CrossRef](#)]
2. Rattan, V.K.; Singh, S.; Sethi, B.P.S. Viscosities, Densities, and Ultrasonic Velocities of binary mixtures, of ethylbenzene, with ethanol, 1-propanol, and 1-butanol at 298.15 and 308.15 K. *J. Chem. Eng. Data* **2004**, *49*, 1074–1077. [[CrossRef](#)]
3. Weng, W.-L. Viscosities and Densities for binary mixtures of anisole with 1-butanol, 1-pentanol, 1-hexanol, 1-heptanol, and 1-octanol. *J. Chem. Eng. Data* **1999**, *44*, 63–66. [[CrossRef](#)]
4. Mahajan, A.R.; Mirgane, S.R. Excess molar volumes and viscosities for binary mixtures of n-octane, n-decane, n-dodecane, and n-tetradecane with octan-2-ol at 298.15 K. *J. Thermodynamics* **2013**, *2013*, 571918. [[CrossRef](#)]
5. Oswal, S.; Patel, A.T. Speeds of sound, isentropic compressibilities, and excess volumes of binary mixtures. 1. Tri-n-alkylamines with cyclohexane and benzene. *J. Chem. Eng. Data* **1994**, *39*, 366–371. [[CrossRef](#)]
6. Queimada, A.J.; Marrucho, I.M.; Coutinho, A.P.; Stenby, E.H. Viscosity and liquid density of asymmetric n-alkane mixtures: Measurement and modeling. *Int. J. Thermophysics* **2005**, *26*, 47–61. [[CrossRef](#)]
7. Podapangi, S.K.; Mancini, L.; Xu, J.; Reddy, S.H.; Di Carlo, A.; Brown, T.M.; Zanotti, G. Green anisole solvent-based synthesis and deposition of phthalocyanine dopant-free hole-transport materials for perovskite solar cells. *Energies* **2023**, *16*, 3643. [[CrossRef](#)]
8. Larson, C.; Lundberg, P.; Tang, S.; Ràfols-Ribé, J.; Sandström, A.; Lindh, E.M.; Wang, J.; Edman, L. A tool for identifying green solvents for printed electronics. *Nat. Commun.* **2021**, *12*, 4510. [[CrossRef](#)]
9. Sekhar, M.C.; Venkatesulu, A.; Gowrisankar, M.; Krishna, T.S. Thermodynamic study of interaction in binary liquid mixture of 2-chloroaniline with some carboxylic acids. *Phys. Chem. Liquids* **2016**, *55*, 196–217. [[CrossRef](#)]
10. Glasstone, S.; Laidler, K.J.; Eyring, H. *The Theory of Rate Processes*; McGraw-Hill: New York, NY, USA, 1941; p. 345.
11. Redlich, O.; Kister, A.T. Thermodynamics of nonelectrolyte solutions, algebraic representation of thermodynamic properties and the classification of solutions. *Ing. Eng. Chem.* **1948**, *40*, 345–348. [[CrossRef](#)]
12. Moravkova, L.; Wagner, Z.; Sedlakova, Z.; Linek, J. Volumetric behavior of binary and ternary liquid systems composed of ethanol, isooctane, and toluene at temperatures from (298.15 to 328.15) K. Experimental data and correlation. *J. Chem. Thermodyn.* **2011**, *43*, 1906–1916. [[CrossRef](#)]
13. McLinden, M.O.; Splett, J.D. A liquid density standard over wide ranges of temperature and pressure based on toluene. *J. Res. Natl. Inst. Stand. Technol.* **2008**, *113*, 29–67. [[CrossRef](#)] [[PubMed](#)]
14. Riddick, J.A.; Bunger, W.B. *Organic Solvents*, 3rd ed.; Wiley-Interscience: New York, NY, USA, 1970; Volume 2.
15. Desyatnyk, O.; Pszczolkowski, L.; Thorwirth, S.; Krygowski, T.M.; Z Kisiel, Z. The rotational spectra, electric dipole moments and molecular structures of anisole and benzaldehyde. *Phys. Chem. Chem. Phys.* **2005**, *7*, 1708–1715. [[CrossRef](#)]
16. Ortega, J. Densities and refractive indices of pure alcohols as a function of temperature. *J. Chem. Eng. Data* **1982**, *27*, 312–317. [[CrossRef](#)]
17. Gonzalez, B.; Dominguez, I.; Gonzalez, E.J.; Dominguez, A. Density, speed of sound, and refractive index of binary systems cyclohexane (1) or methylcyclohexane (1) or cyclooctane (1) with benzene (2), toluene (2), and ethylbenzene (2) at two temperatures. *J. Chem. Eng. Data* **2010**, *55*, 1003–1011. [[CrossRef](#)]
18. Baragi, J.G.; Aralaguppi, M.I.; Aminabhavi, T.M.; Kariduraganavar, M.Y.; Kittur, A.A. Density, viscosity, refractive index, and the speed of sound for binary mixtures of anisole with 2-chloroethanol, 1,4-dioxane, tetrachloroethylene, tetrachloroethane, DMF, DMSO, and diethyl oxalate at (298.15, 303.15, and 308.15) K. *J. Chem. Eng. Data* **2005**, *50*, 910–916. [[CrossRef](#)]
19. Wei, I.C.; Rowley, R.L. Binary liquid mixture viscosities and densities. *J. Chem. Eng. Data* **1984**, *29*, 332. [[CrossRef](#)]
20. Krall, A.H.; Sengers, J.V.; Kestin, J. Viscosity of liquid toluene at temperatures from 25 to 150 °C and at pressures up to 30 MPa. *J. Chem. Eng. Data* **1992**, *37*, 349–355. [[CrossRef](#)]
21. Fort, R.J.; Moore, W.R. Adiabatic compressibilities of binary mixtures. *Trans. Faraday Soc.* **1965**, *61*, 2102–2111. [[CrossRef](#)]
22. Jorge, M.; Gomes, J.R.B.; Barrera, M.C. Dipole moments of alcohols in the liquid phase and in solution. *J. Mol. Liq.* **2022**, *356*, 11903. [[CrossRef](#)]
23. Vaughan, W.E. Digest of literature on dielectrics. *Natl. Acad. Sci.* **1969**, *33*, 21.
24. Chirico, R.D.; Frenkel, M.; Diky, V.V.; Marsh, K.N.; Wilhoit, R.C. ThermoML—an XML-based approach for the storage and exchange of experimental and critically evaluated thermophysical and thermochemical property data. 2. Uncertainties. *J. Chem. Eng. Data* **2003**, *48*, 1344–1359. [[CrossRef](#)]
25. Iglesias, T.P.; Legido, J.L.; Pereira, S.M.; de Cominges, B.; Andrade, M.I.P. Relative permittivities and refractive indices on mixing for (n-hexane + 1-pentanol, or 1-hexanol or 1-heptanol) at 298.15 K. *J. Chem. Thermodyn.* **2000**, *32*, 923–930. [[CrossRef](#)]
26. Ocon, J.; Tojo, G.; Espada, L. *An. Quim* **1969**, *65*, 1641 as quoted by Srivastava, R.; Smith, B.D. Evaluation of binary excess volume data for methanol and hydrocarbon systems. *J. Phys. Chem. Ref. Data* **1987**, *16*, 209–218.
27. Letcher, T.M.; Prasad, A.L.; Mercer-Chalmers, J. Excess molar enthalpies and excess molar volumes on mixing an aromatic compound with an alcohol at 298.15 K. *S. Afr. J. Chem.* **1991**, *44*, 17–21.
28. Nikam, P.S.; Jagdale, B.S.; Saswant, A.B.; Hasan, M. Densities and Viscosities of Binary Mixtures of Toluene with Methanol, Ethanol, Propan-1-ol, Butan-1-ol, Pentan-1-ol, and 2-Methylpropan-2-ol at (303.15, 308.15, 313.15) K. *J. Chem. Eng. Data* **2000**, *45*, 559–563. [[CrossRef](#)]

29. Rodriguez, A.; Canosa, J.; Tojo, J. Density, refractive index and speed of sound of the ternary mixtures (dimethylcarbonate or diethylcarbonate + methanol + toluene and the corresponding binaries at T=298.15 K. *J. Chem. Thermodyn.* **2001**, *33*, 1383–1397. [[CrossRef](#)]
30. Mialkowski, C.; Chagnes, A.; Carre, B.; Lemordant, D.; Willmann, P. Excess thermodynamic properties of binary liquid mixtures containing dimethylcarbonate and  $\gamma$ -butyrolactone. *J. Chem. Thermodyn.* **2002**, *34*, 1847–1856. [[CrossRef](#)]
31. Roy, M.N.; Sinha, A.; Sinha, B. Excess molar volumes, viscosity deviations, and isentropic compressibility of binary mixtures containing 1,3-dioxolane, and monoalcohols at 303.15 K. *J. Solut. Chem.* **2005**, *34*, 1311–1325. [[CrossRef](#)]
32. Baluja, S.; Oza, S. Studies of some acoustical properties in binary solutions. *Fluid Phase Equilib.* **2001**, *178*, 233–238. [[CrossRef](#)]
33. Prolongo, M.G.; Masegosa, R.M.; Hernandez-Fuentes, I. Viscosities and excess volumes of binary mixtures formed by the liquids acetonitrile, pentyl acetate, 1-chlorobutane, and carbon tetrachloride at 25 °C. *J. Phys. Chem.* **1984**, *88*, 2163–2167. [[CrossRef](#)]
34. Aminabhavi, V.A.; Aminabhavi, T.M.; Balundgi, R.H. Evaluation of excess parameters from density and viscosities of binary mixtures of ethanol with anisole, N, N-dimethylformamide, carbon tetrachloride, and acetophenone from 298.15 K to 313.15 K. *Ind. Eng. Chem. Res.* **1990**, *29*, 2106–2111. [[CrossRef](#)]
35. Parks, G.S.; Moore, G.E.; Renquist, M.L.; Naylor, B.F.; McClaine, L.A.; Fujii, P.S.; Hatton, J.A. Thermal data on organic compounds. XXV. Some heat capacity, entropy and free energy data for nine hydrocarbons of high molecular weight. *J. Am. Chem. Soc.* **1949**, *71*, 3386–3389. [[CrossRef](#)]
36. Nath, J.; Dubey, S.N. Binary systems of trichloroethylene with benzene, toluene, p-xylene, carbon tetrachloride, and chloroform. Ultrasonic velocities and adiabatic compressibilities at 303.15 and 313.15 K, and dielectric properties and refractive indexes at 303.15 K. *J. Phys. Chem.* **1980**, *84*, 2166–2170. [[CrossRef](#)]

**Disclaimer/Publisher's Note:** The statements, opinions and data contained in all publications are solely those of the individual author(s) and contributor(s) and not of MDPI and/or the editor(s). MDPI and/or the editor(s) disclaim responsibility for any injury to people or property resulting from any ideas, methods, instructions or products referred to in the content.